Supporting Information for "Sensitivity of GNSS-Derived Estimates of Terrestrial Water Storage to Assumed Earth Structure"

Matthew J. Swarr[1], Hilary R. Martens[1], and Yuning Fu[2]

[1]Department of Geosciences, University of Montana, Missoula, MT, USA

[2]School of Earth, Environment, and Society, Bowling Green State University, Bowling Green, OH, USA

Contents of this file

Additional Supporting Information (Files uploaded separately)

Region	Sampling Location	Local Lithosphere Thickness [km]
San Joaquin River Basin	39.792° N, −121.604° W	54.553
Sacramento River Basin	37.686° N, −120.475° W	54.679
Tulare River Basin	36.155° N, −119.409° W	76.14
Northern Sierra Nevada	39.612° N, −120.879° W	50.892
Central Sierra Nevada	38.102° N, −119.864° W	51.789
Southern Sierra Nevada	36.476° N, −118.496° W	68.309
Northern Cascades	48.404° N, −121.234° W	53.937
Central Cascades	45.399° N, −121.759° W	54.491
Southern Cascades	41.014° N, −122.118° W	61.983

Table S1. Sampling locations and local lithosphere thickness of radial profiles derived from LITHO1.0 used compute the average local crust and upper mantle structure of the SST River Basin, Sierra Nevada, and Cascade Range respectively.

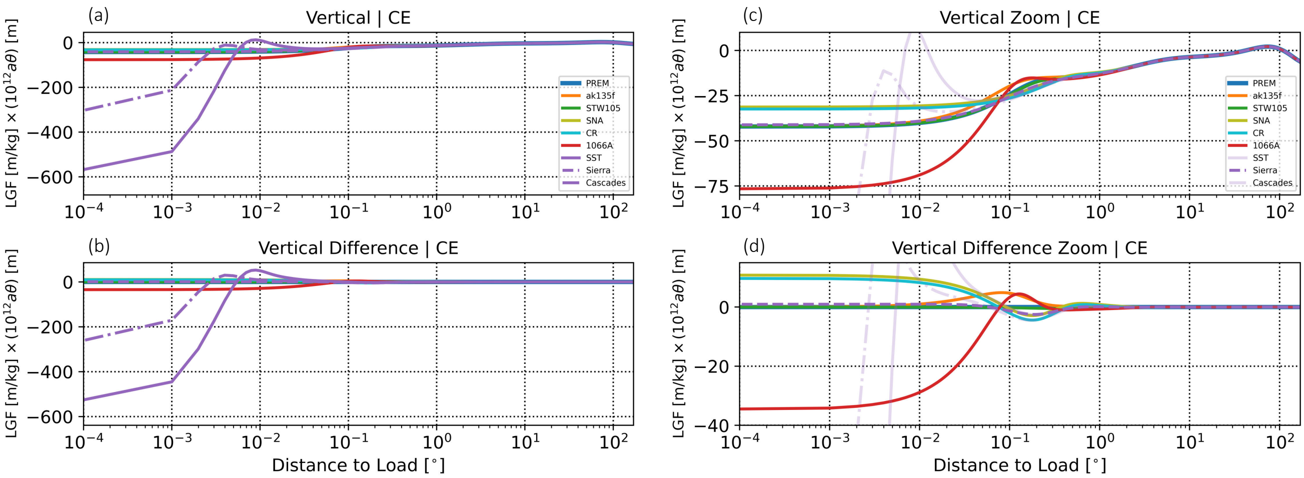

Figure S1. Displacement load Green's functions computed in the CE reference frame for PREM (blue), AK135f (orange), STW105 (green), SNA (olive), CR (cyan), 1066A (red), and average crust and upper mantle models for the San Joaquin, Sacramento, Tulare River Basin (purple), Sierra Nevada (dashed purple), and the Cascade Range (dash-dot purple). Panel (a) displays the vertical-component of the LGFs over angular distances that range from 0.001° to 170° respectively. The LGFs have been multiplied by a scaling factor $10^{12}a\theta$, where a is Earth's mean radius (units of meters) and θ represents the angular distance between the applied load and the point of observation (units of radians). Panel (b) displays the LGFs of the models considered here relative to the LGFs of PREM. Panels (c) and (d) depict a zoomed in version of the information depicted in (a) and (b).

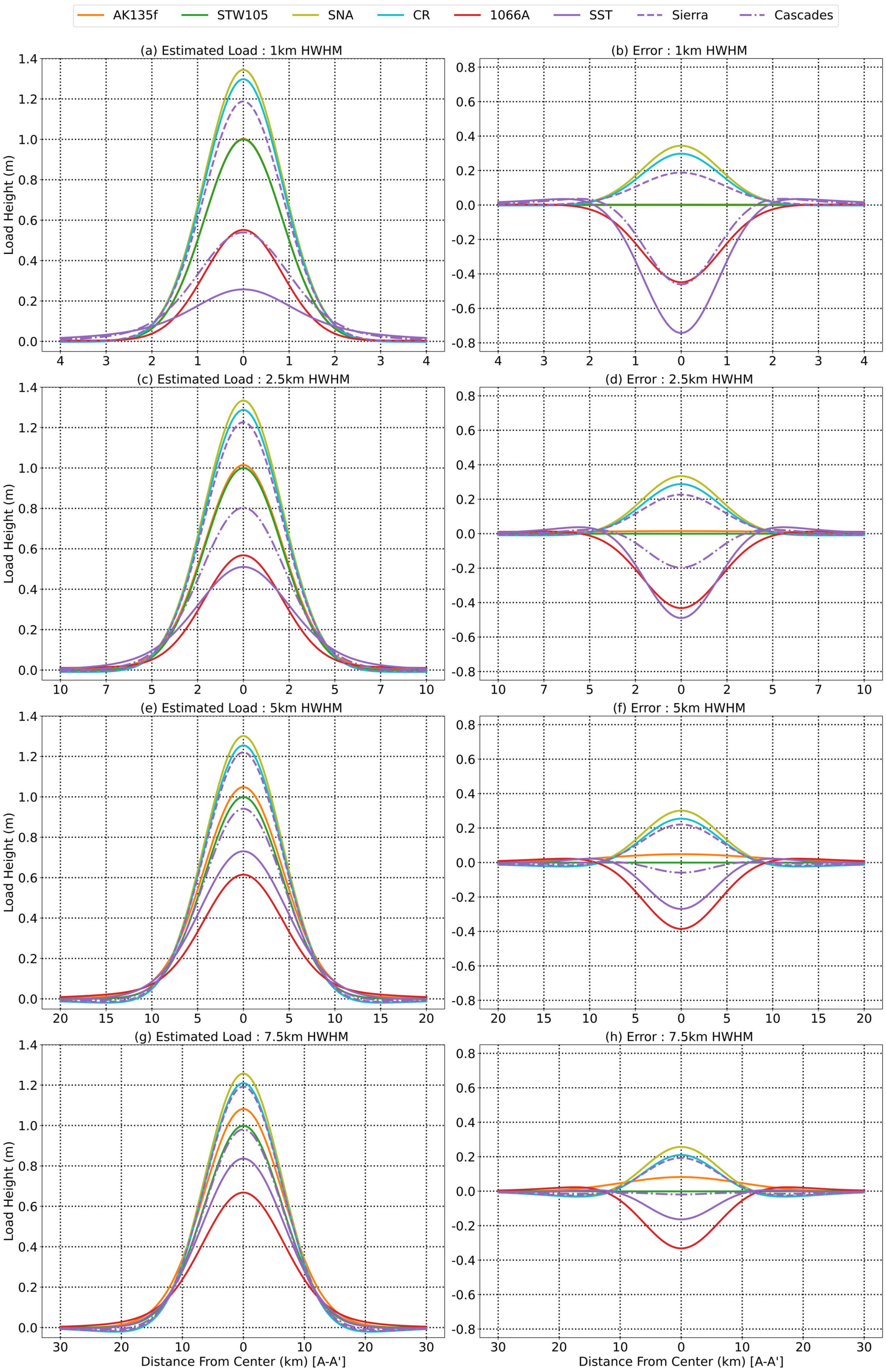

Figure S2. Estimated surface load and associated error for inversion estimates assuming the SNREI Earth structures shown in Fig. 1 along the profile A-A' in Fig. 2 for surface loads corresponding to HWHMs of: (a-b) 1 km, (c-d) 2.5 km, (e-f) 5 km, and (g-h) 7.5 km.

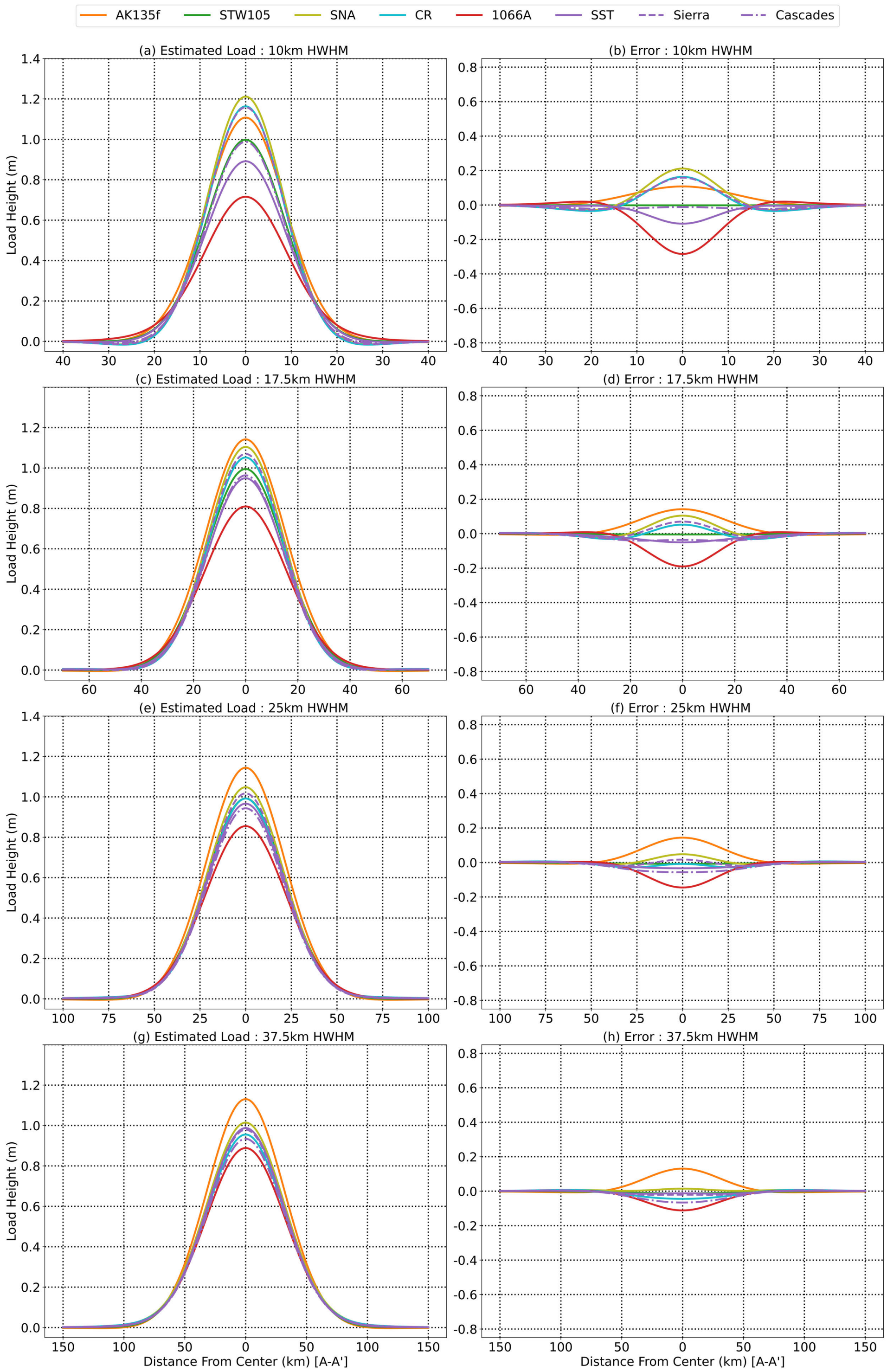

Figure S3. Estimated surface load and associated error for inversion estimates assuming the SNREI Earth structures shown in Fig. 1 along the profile A-A' in Fig. 2 for surface loads corresponding to HWHMs of: (a-b) 10 km, (c-d) 17.5 km, (e-f) 25 km, and (g-h) 37.5 km.

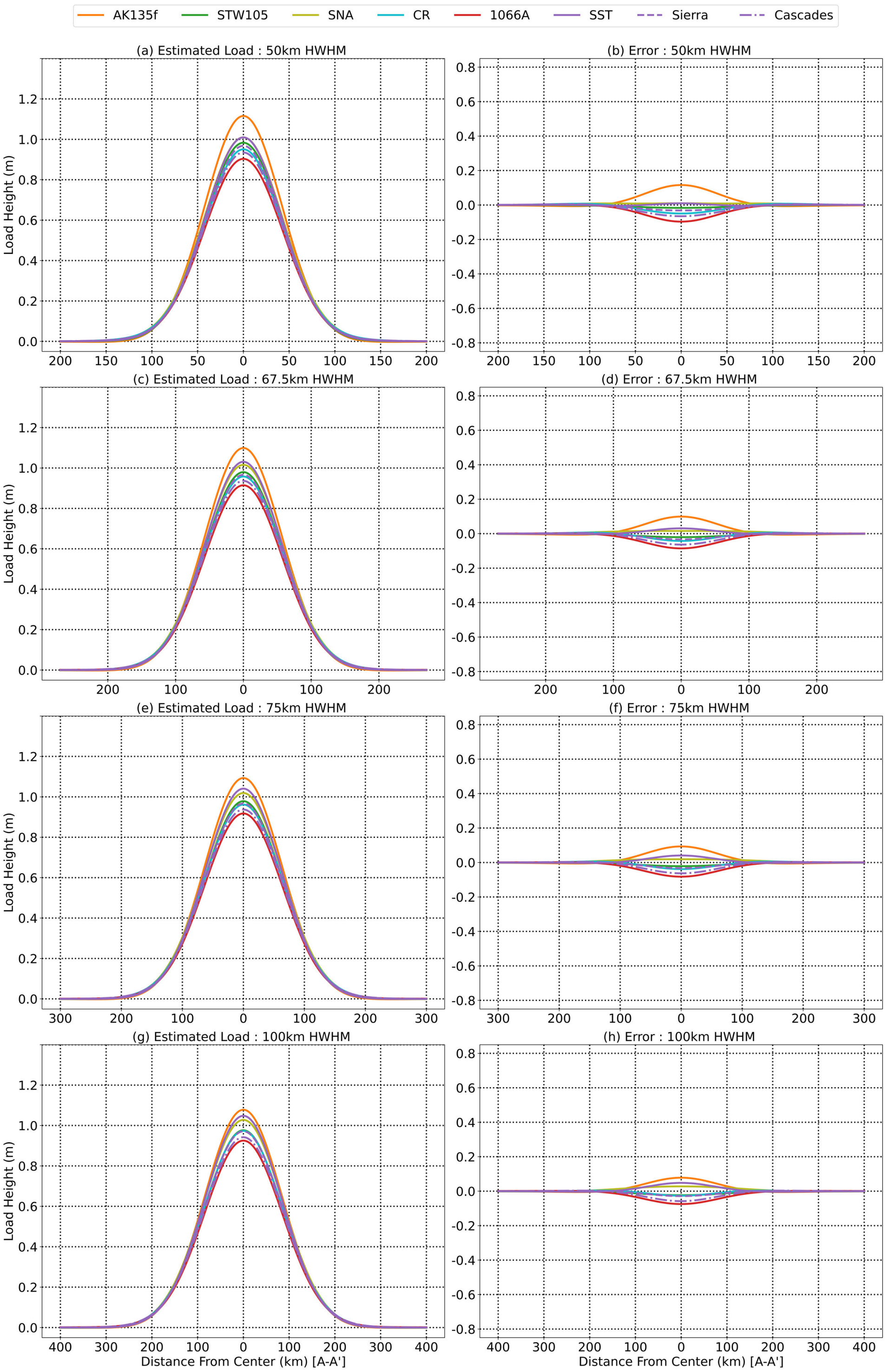

33

34 **Figure S4.** Estimated surface load and associated error for inversion estimates assuming the
35 SNREI Earth structures shown in Fig. 1 along the profile A-A' in Fig. 2 for surface loads
36 corresponding to HWHMs of: (a-b) 50 km, (c-d) 67.5 km, (e-f) 75 km, and (g-h) 100 km.

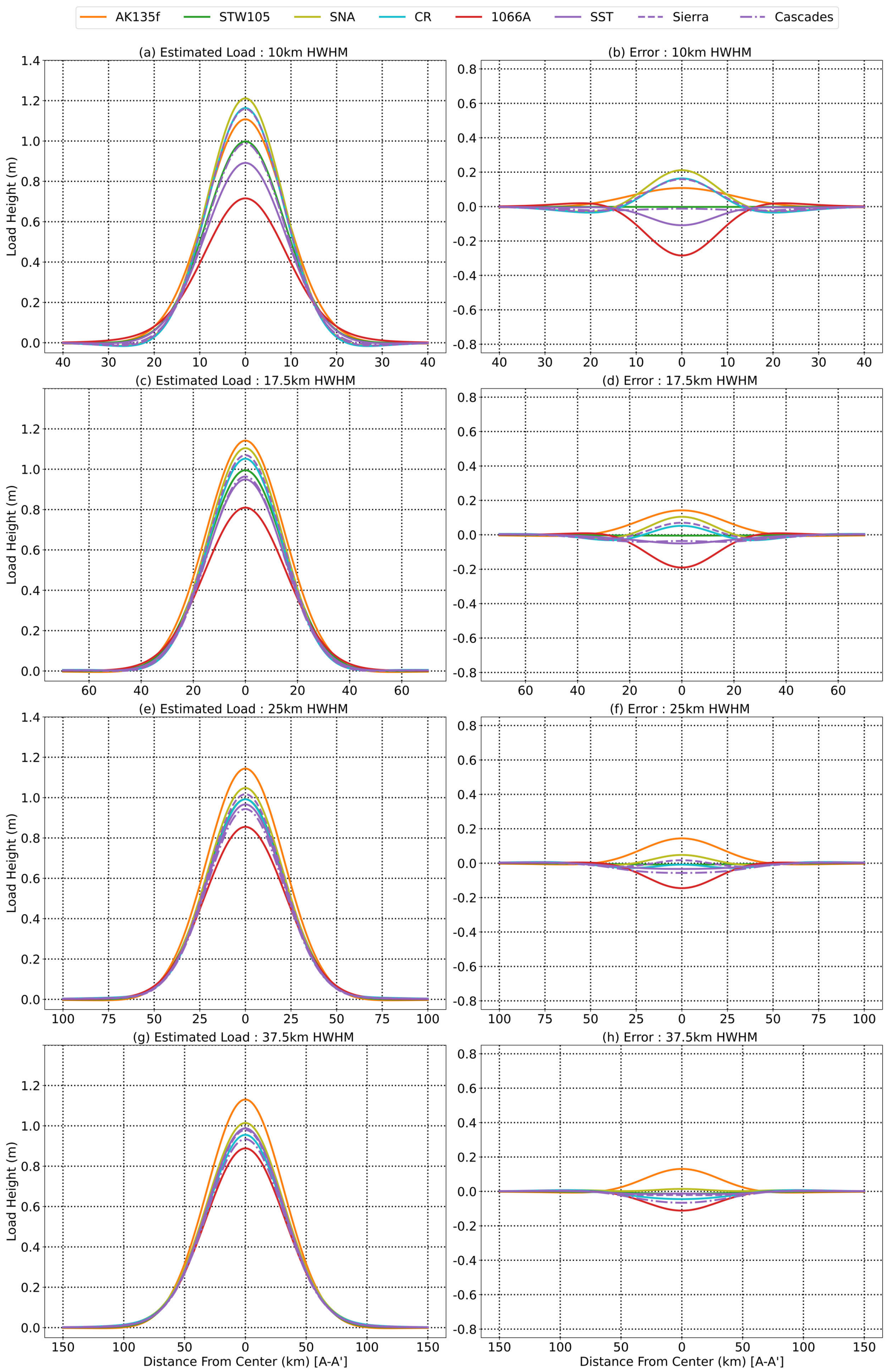

38 **Figure S5.** Estimated surface load and associated error for inversion estimates assuming the SNREI Earth structures shown in Fig. 1 along the profile A-A' in Fig. 2 for surface loads corresponding to HWHMs of: (a-b) 175 km, (c-d) 250 km, (e-f) 500 km, and (g-h) 750 km.

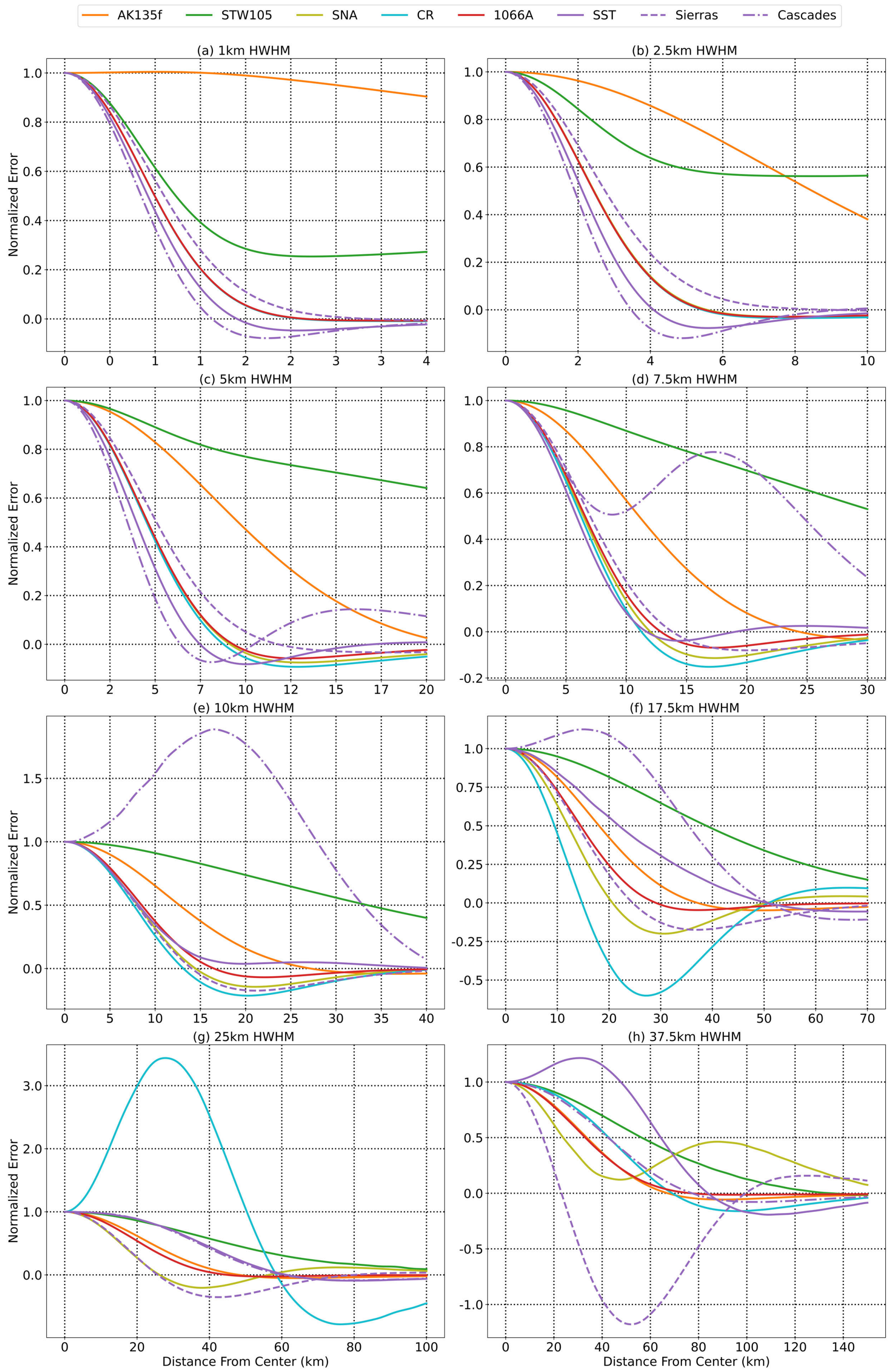

41

42 **Figure S6.** Error is estimated surface load normalized by the misfit at the center of the load

43 for surface loads corresponding to HWHMs between 1 and 37.5 km.

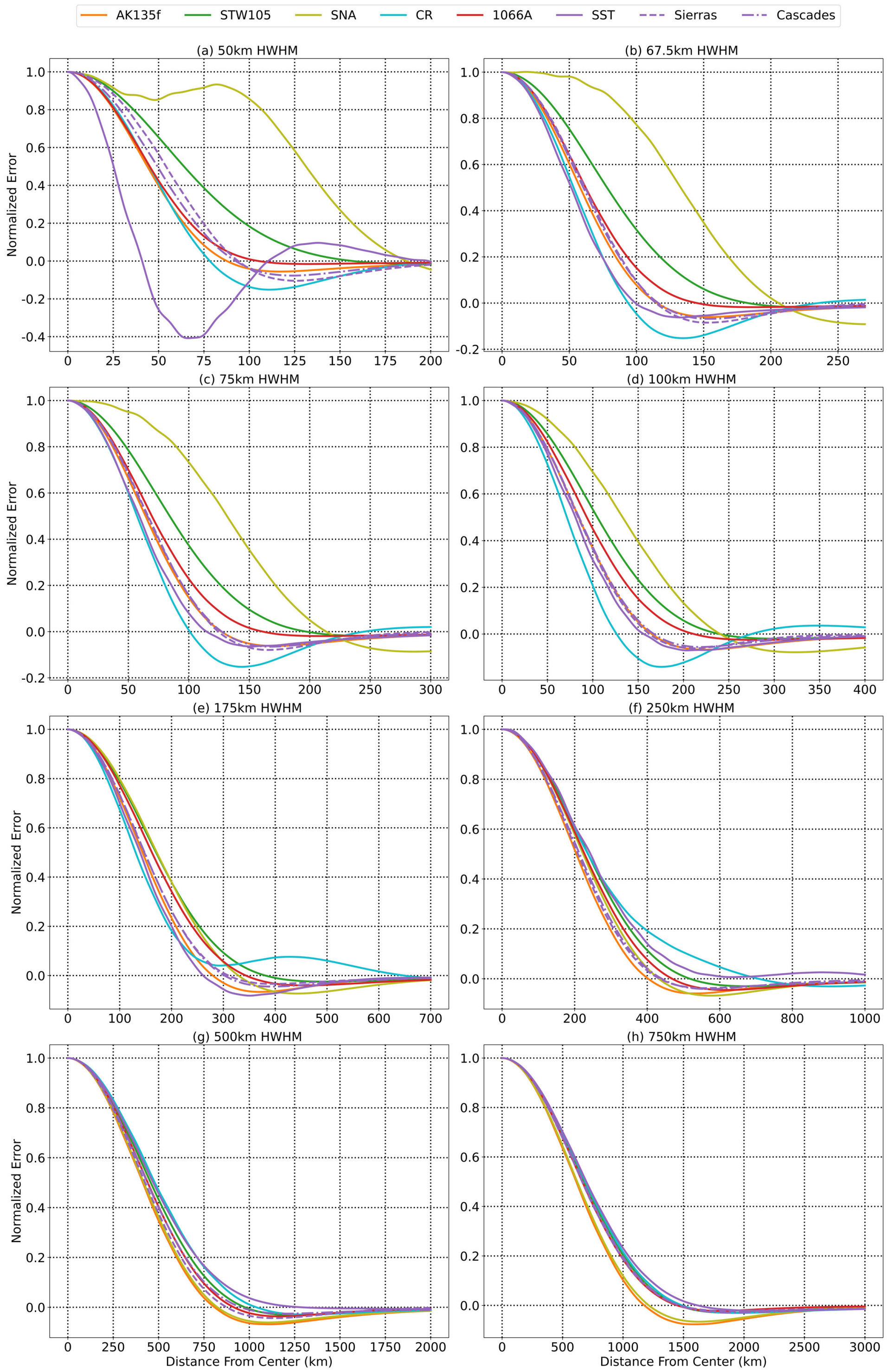

44

45 **Figure S7.** Error is estimated surface load normalized by the misfit at the center of the load

46 for surface loads corresponding to HWHMs between 50 and 750 km.

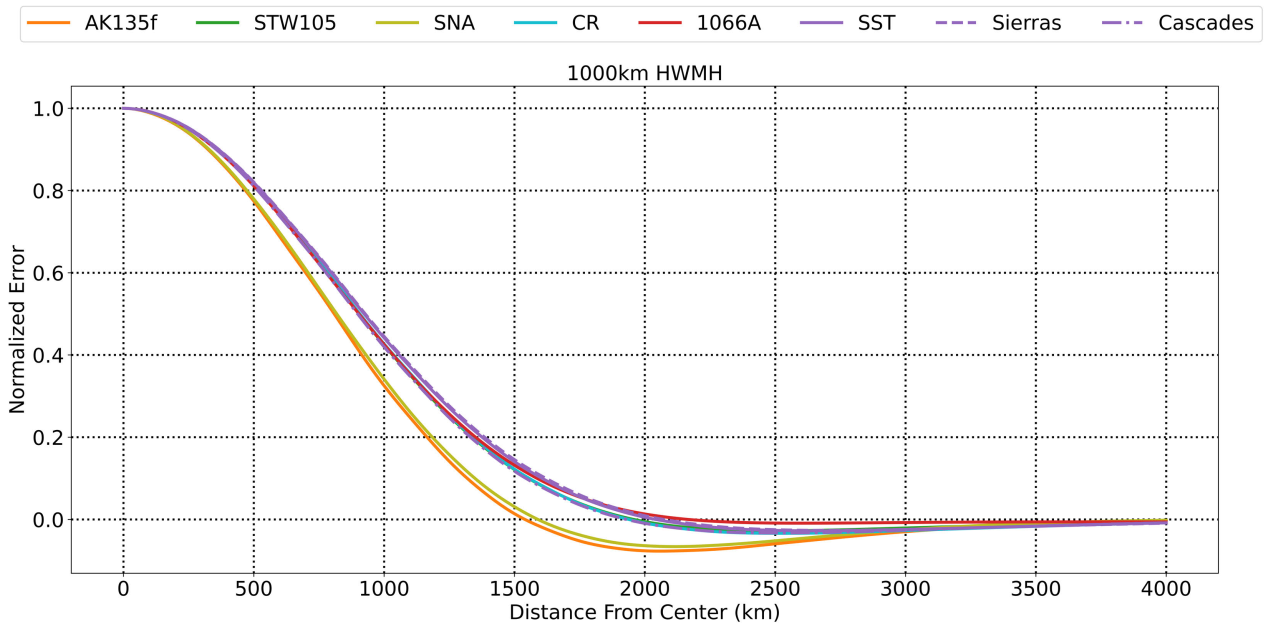

Figure S8. Error is estimated surface load normalized by the misfit at the center of the load for a surface loads with a HWHM of 1000 km.

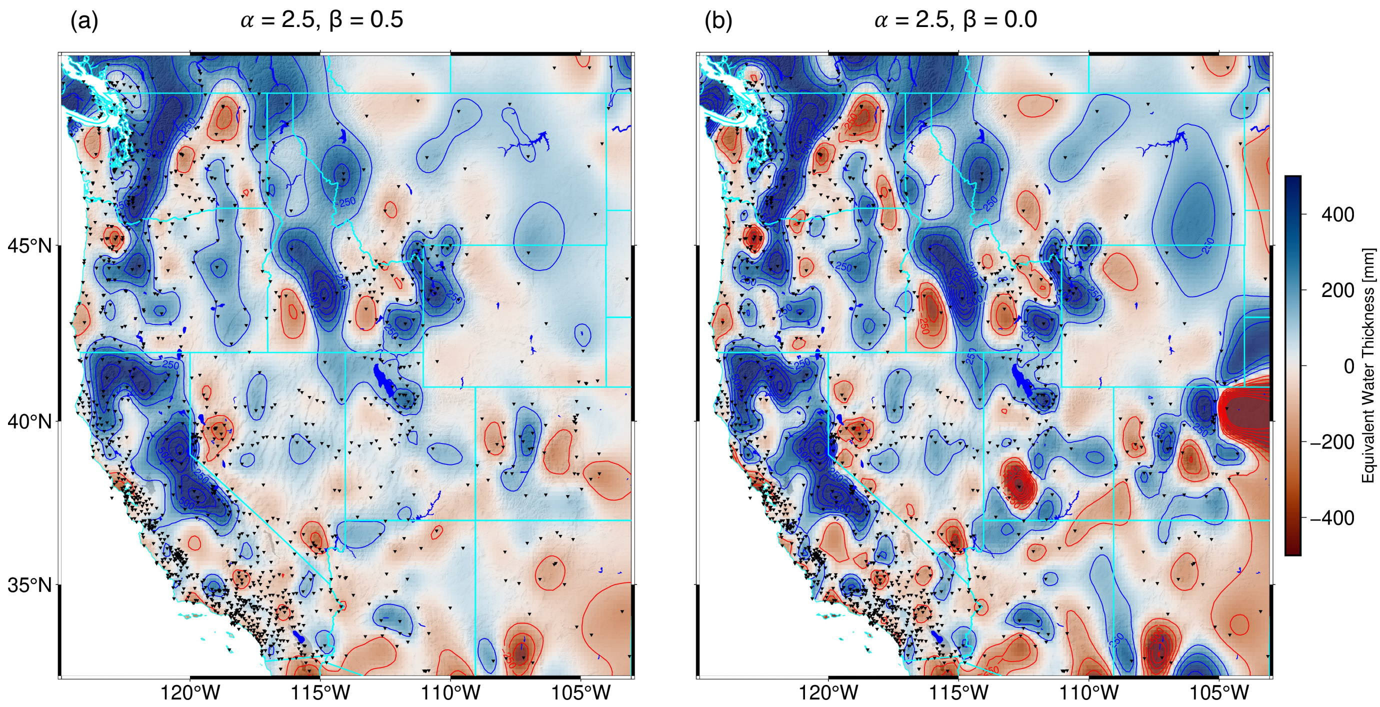

Figure S9. Estimated seasonal change in storage for the month of April 2017. (1) estimates produced using eq.2 (b) estimates produced using equation eq.1 which yield large gains/losses in the eastern portion of our model domain. Units are meter of equivalent water thickness. Contours represent 250 mm of water loss/gain.

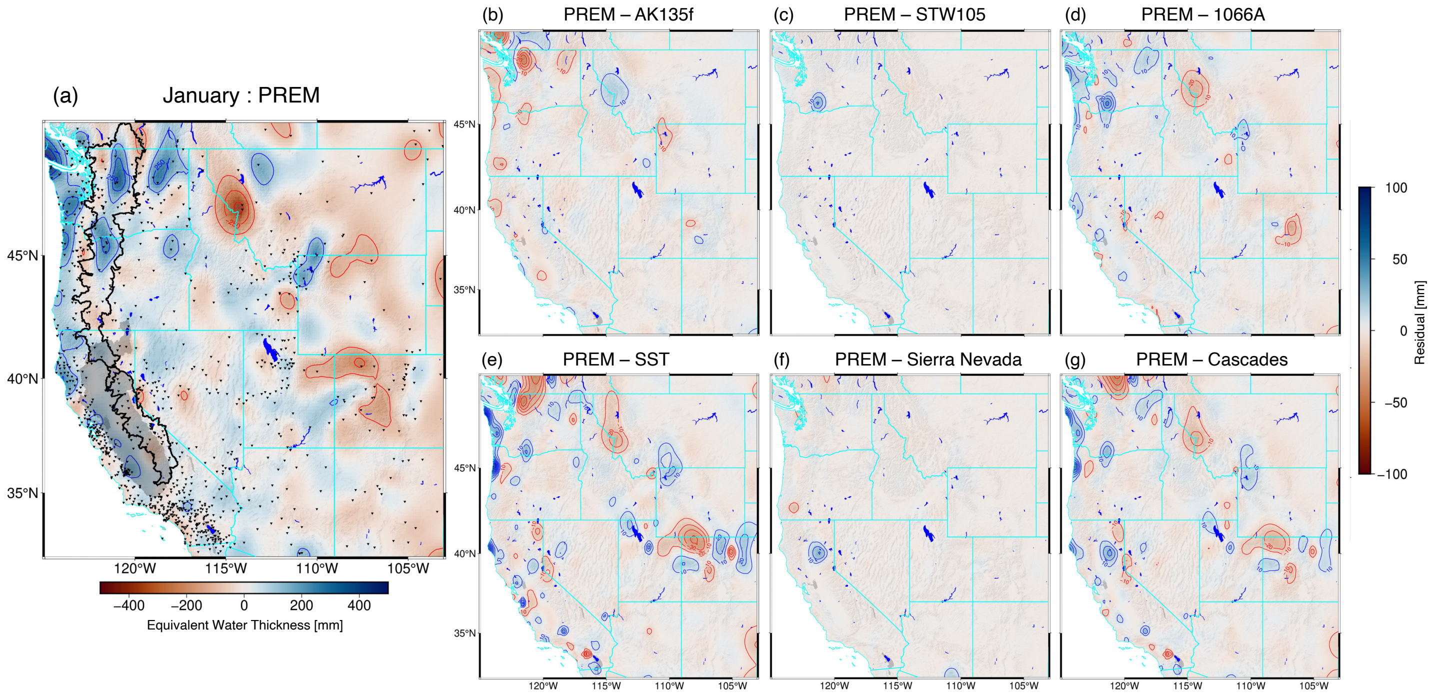

Figure S10. a) Multi-year monthly stacked estimate of seasonal change in storage for the month of January. Contours represent 125 mm intervals of equivalent water thickness. Direct differences between pairs of TWS estimates for the month of April using select Earth models: (b) PREM and AK135f, (c) PREM and STW105, (d) PREM and 1066A, (e) PREM and LITHO1.0 model for the SST River Basin, (f) PREM and LITHO1.0 model for the Sierra Nevada, and (g) PREM and LITHO1.0 model for the Cascade Range. The color bars at right denotes the amplitude of the residuals between TWS estimates. Contours represent 10 mm residual intervals of equivalent water thickness.

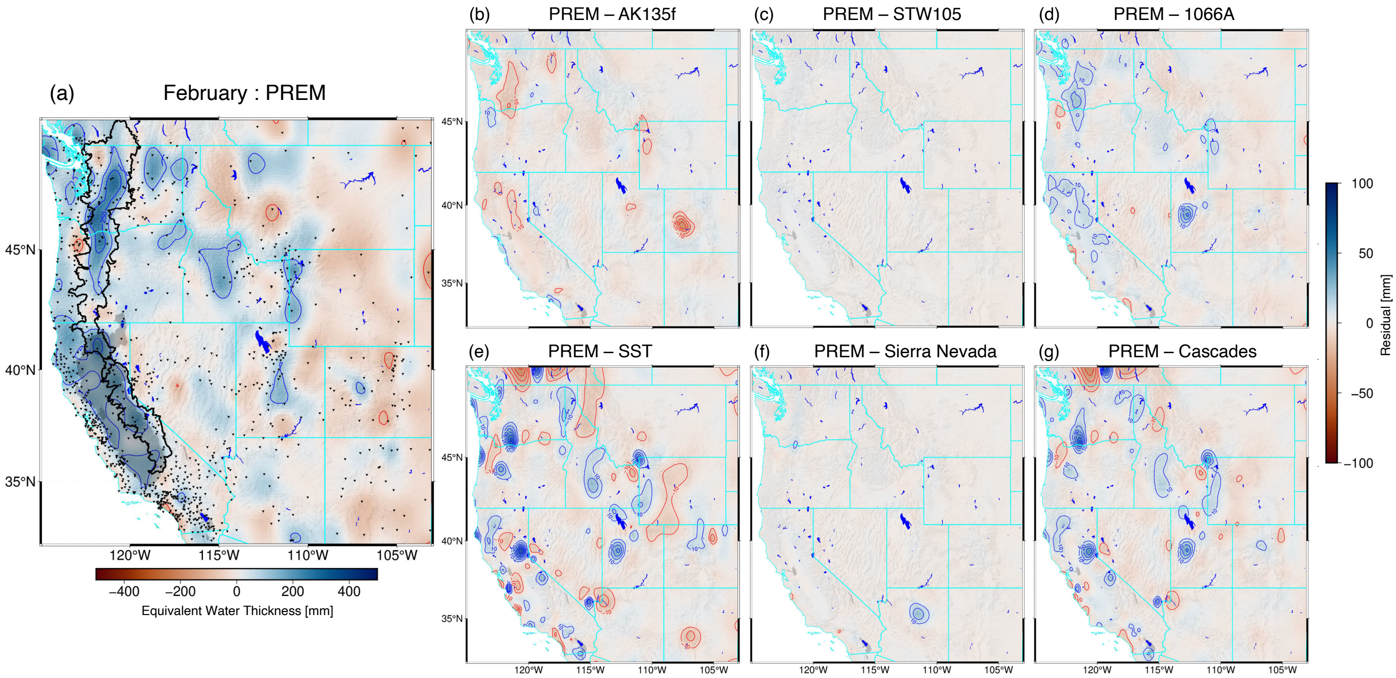

Figure S11. a) Multi-year monthly stacked estimate of seasonal change in storage for the month of February.

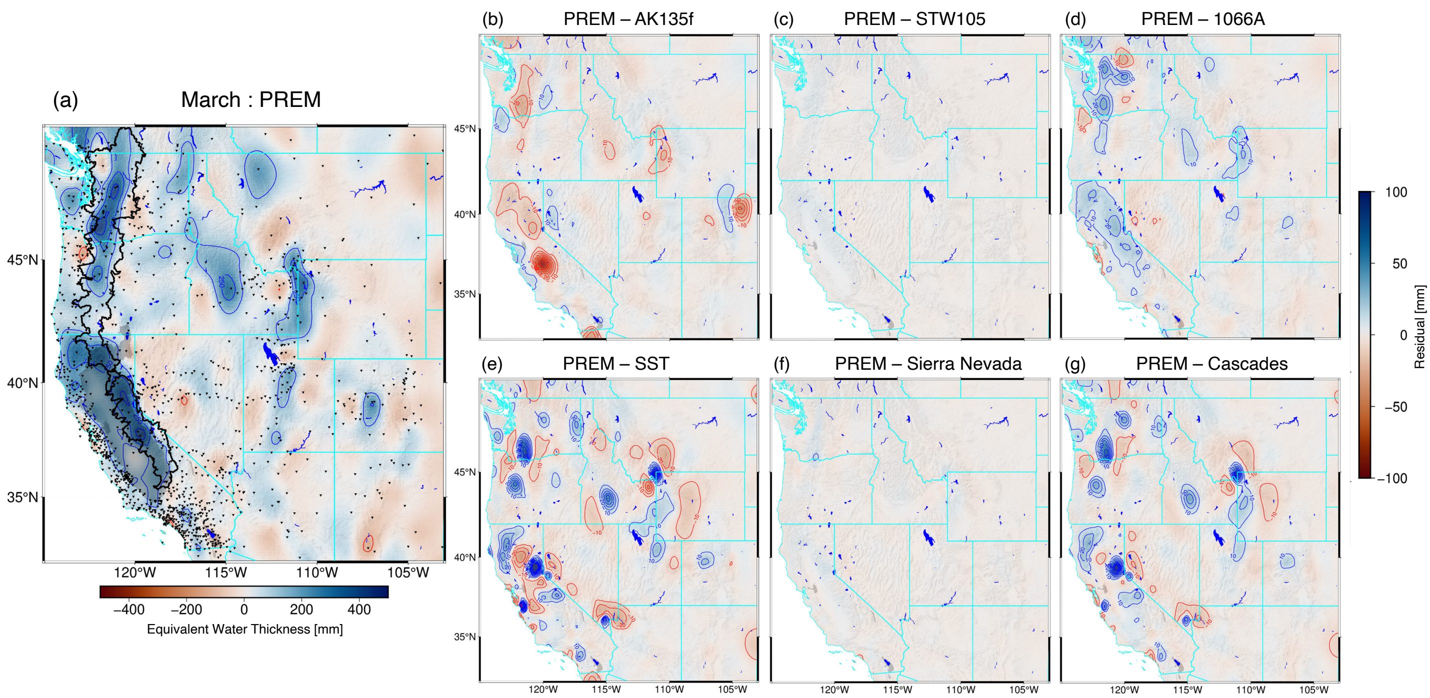

Figure S12. a) Multi-year monthly stacked estimate of seasonal change in storage for the month of March.

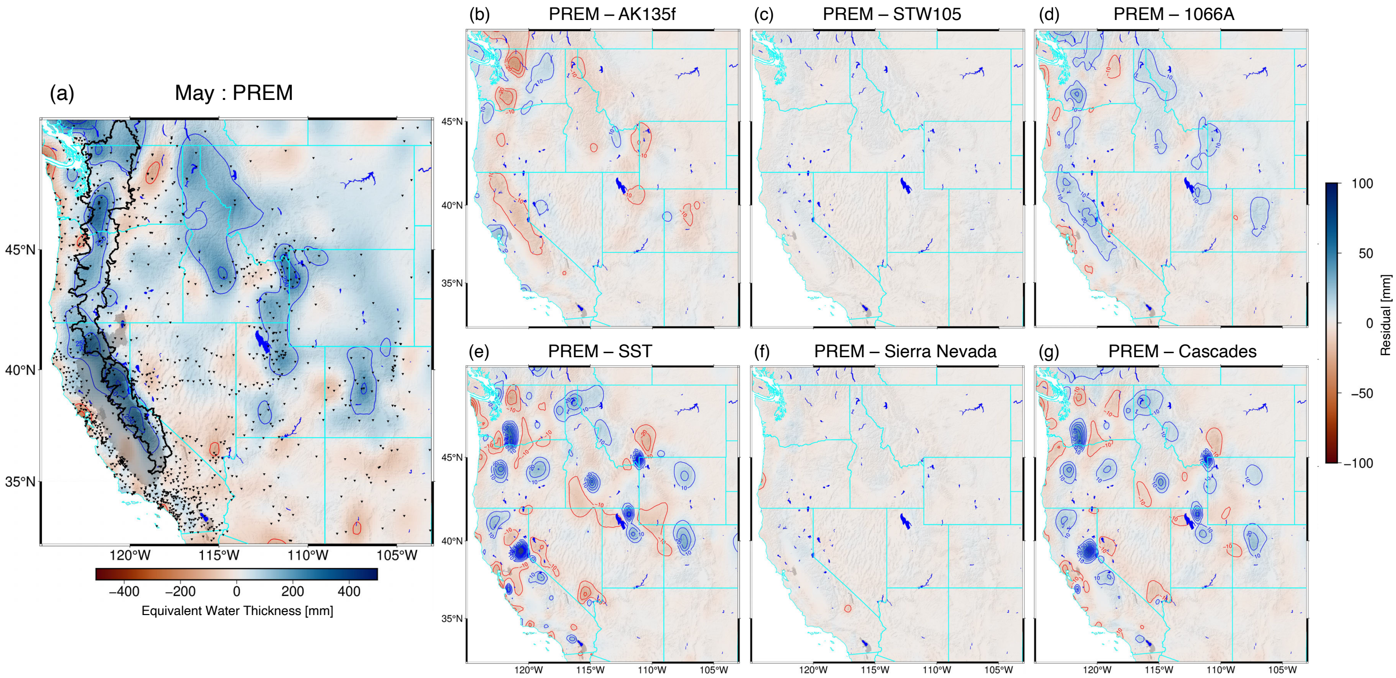

Figure S13. a) Multi-year monthly stacked estimate of seasonal change in storage for the month of May.

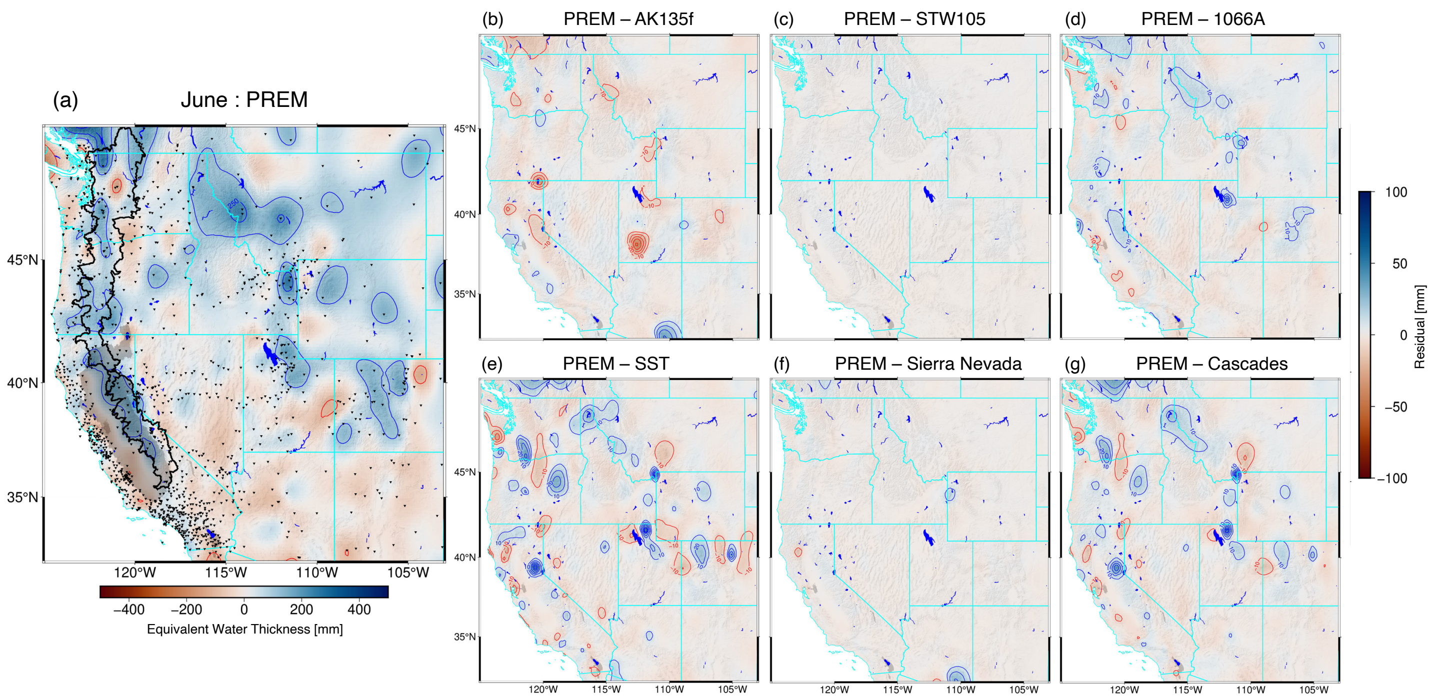

Figure S14. a) Multi-year monthly stacked estimate of seasonal change in storage for the month of June.

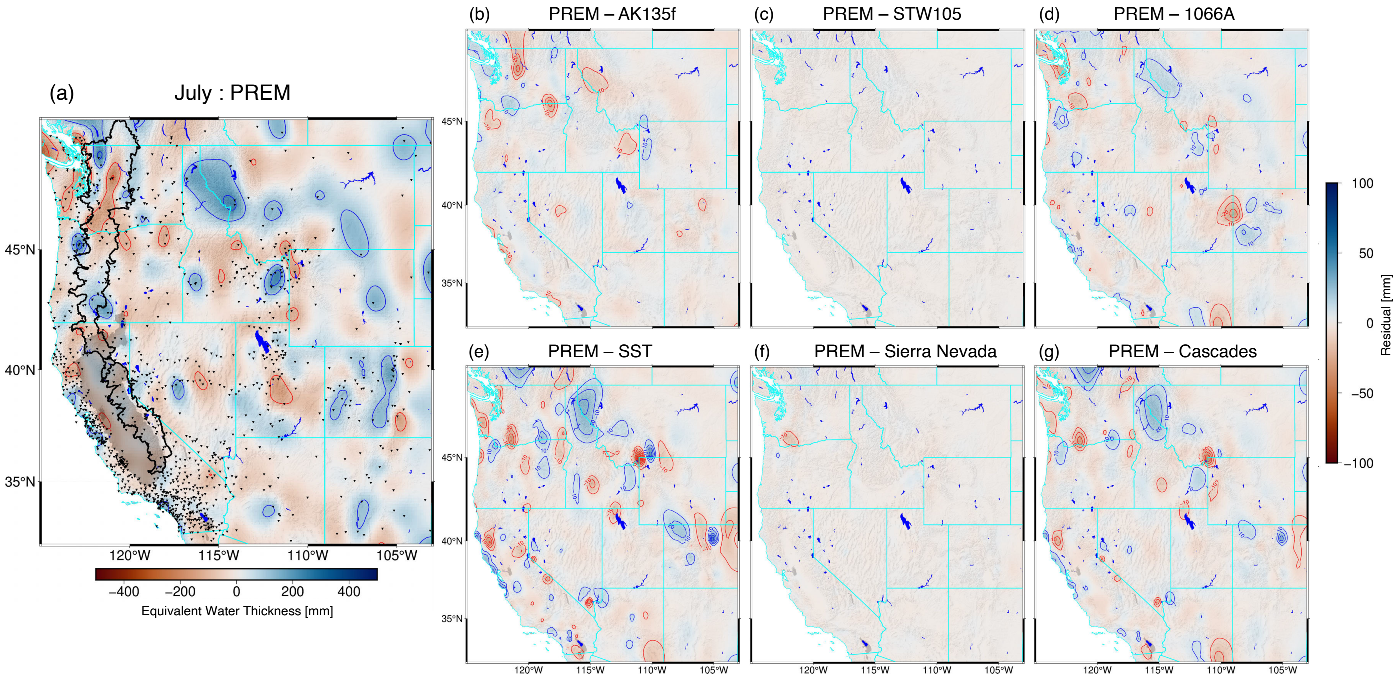

Figure S15. a) Multi-year monthly stacked estimate of seasonal change in storage for the month of July.

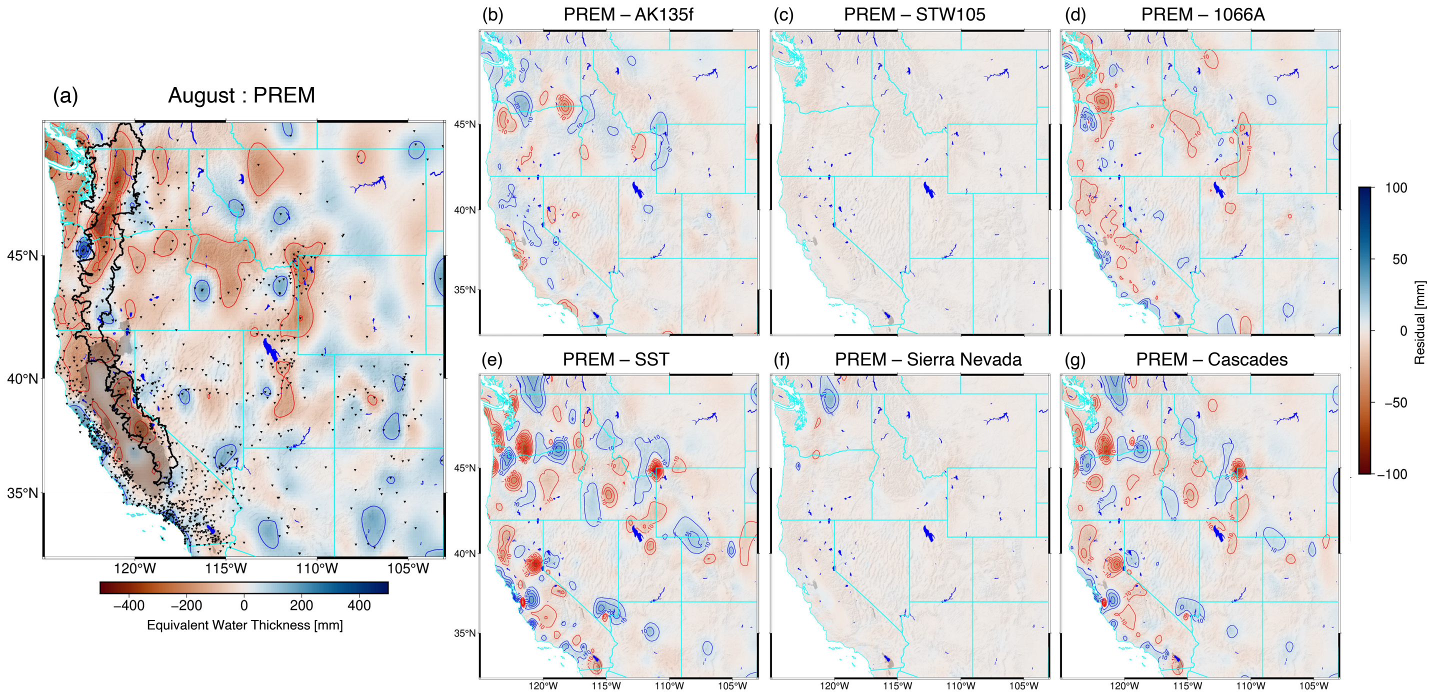

Figure S16. a) Multi-year monthly stacked estimate of seasonal change in storage for the month of August.

90

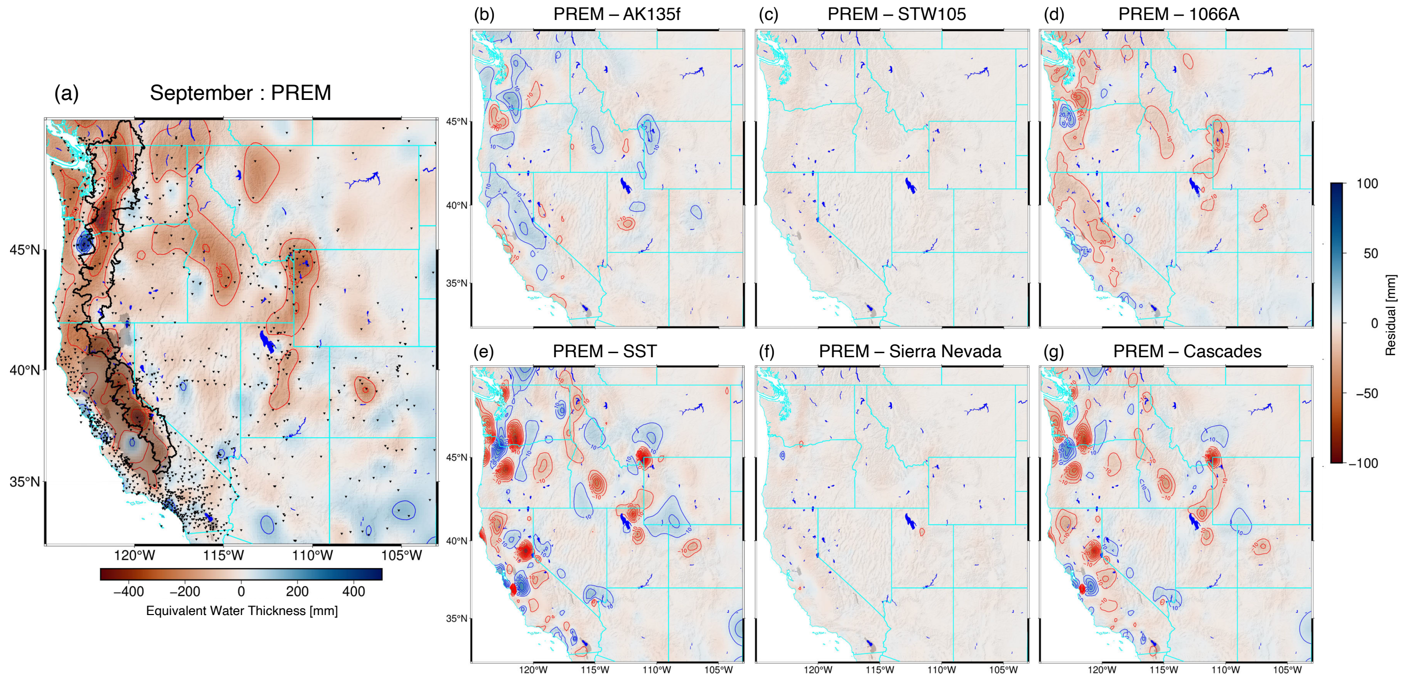

91

92 **Figure S17.** a) Multi-year monthly stacked estimate of seasonal change in storage for the month

93 of September.

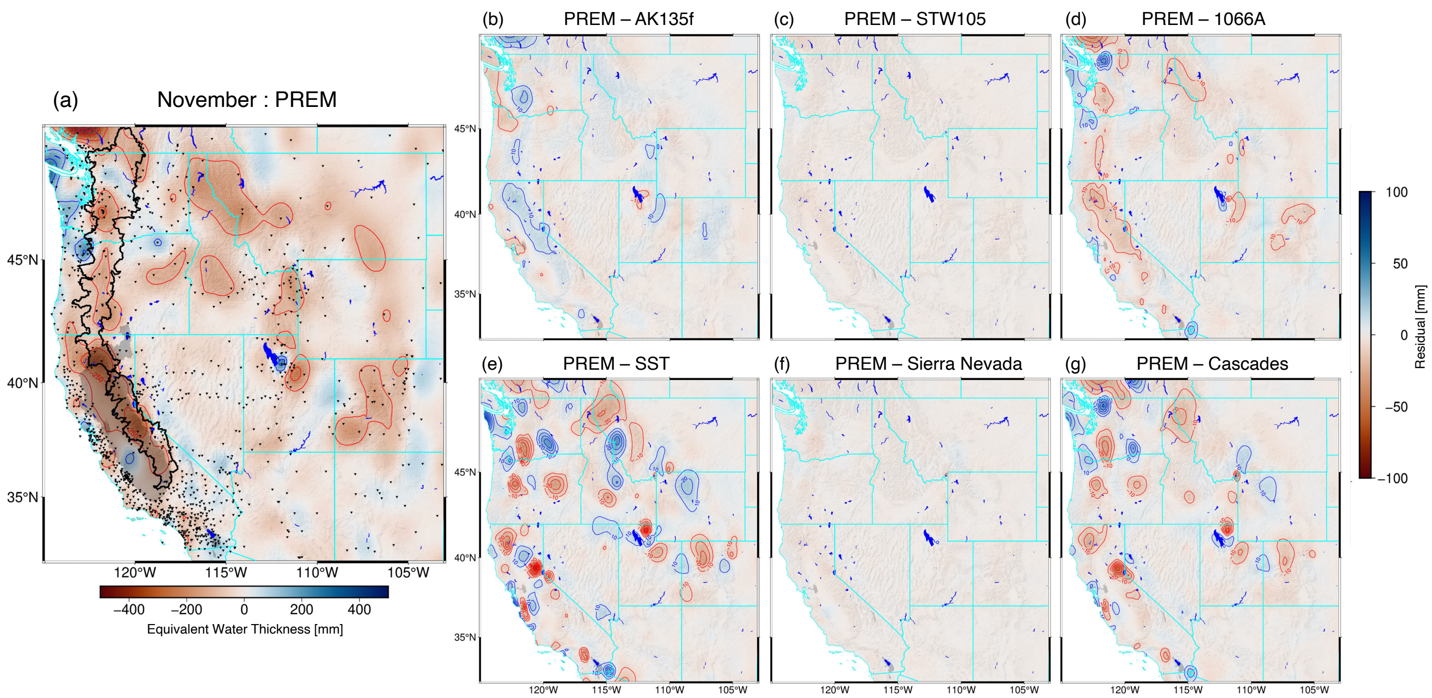

Figure S18. a) Multi-year monthly stacked estimate of seasonal change in storage for the month of November.

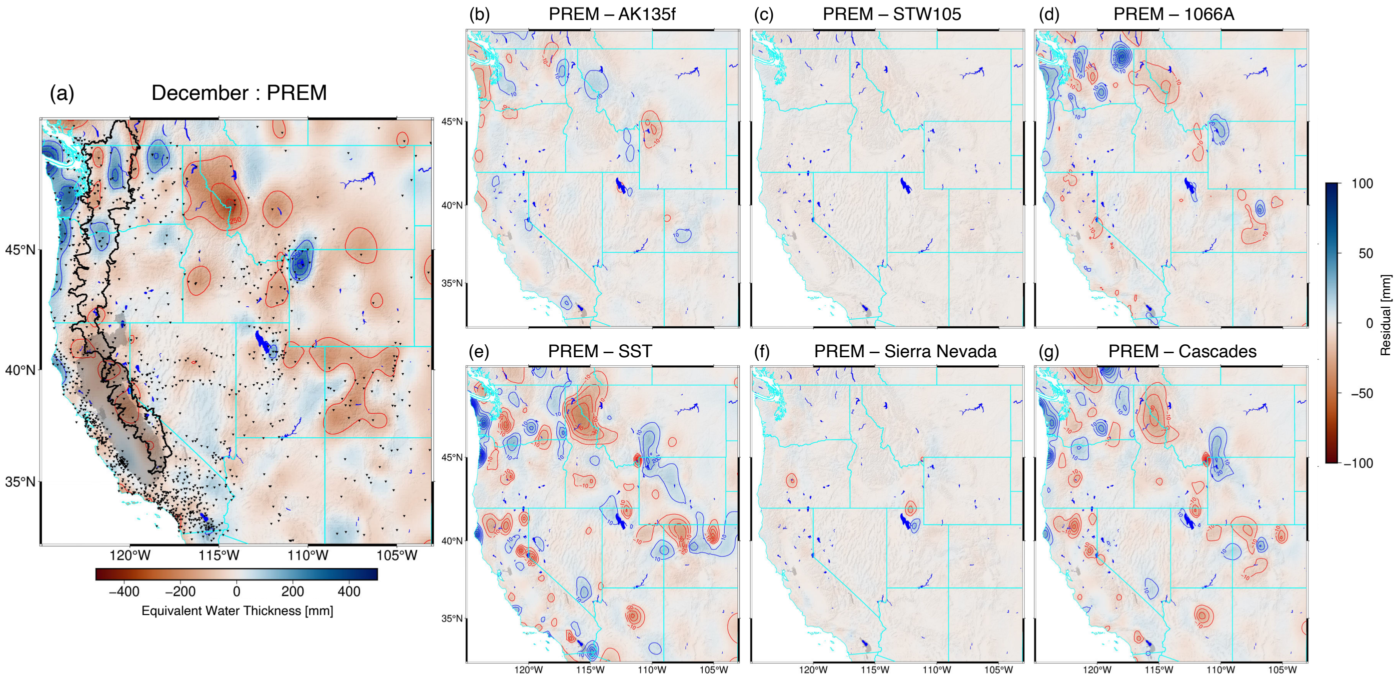

Figure S19. a) Multi-year monthly stacked estimate of seasonal change in storage for the month of December.

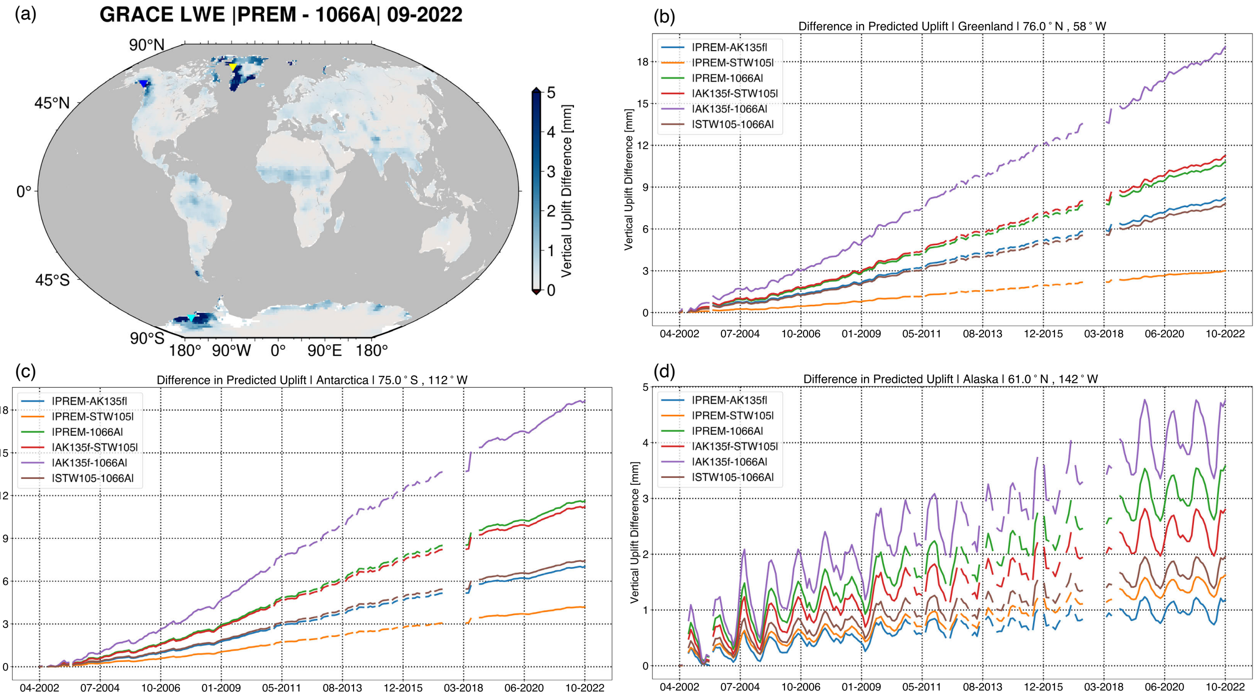

Figure S20. a) Amplitude of the difference in predicted VLM between predictions derived from PREM and 1066A for the month of September 2022. Inverted triangles represent sampling locations for the time series of VLM depicted in panels (b-d). Difference in predicted VLM between April 2002 and September 2022 for select Earth models at : (b) 76.0° N, 58° W on the western portion of the Greenland Ice Sheet, (c) 75° S, 112° W in western Antarctica, and (d) 61.0° N, 142° W in southeastern Alaska. Gaps in predicted VLM depicted here represent data gaps in the time series of GRACE and GRACE-FO.

Dataset S1. Final stations used to invert observed vertical displacements within the western U.S. to estimate seasonal changes in terrestrial water storage within the region between January 2006 and September 2022. The steps followed to determine the final set of stations used in this study are described in the main text of this manuscript.

Dataset S2. Full dataset of inversion solutions (txt format) and input surface load models used in the synthetic tests section of this work. Each file's name in the data set describes both the size of the load the solution corresponds to and the Earth model used in the design matrix of the inversion.

Dataset S3. Full dataset of inversion solutions (txt format) for seasonal TWS changes in the western U.S. between January 2006 and September 2022. Each file's name indicates the Earth model that used to construct the design matrix of the inversion.